Progress in Nuclear Energy 185 (2025) 105745

Contents lists available at ScienceDirect

Progress in Nuclear Energy

journal homepage: www.elsevier.com/locate/pnucene

# Physics-Informed Neural Networks for the safety analysis of nuclear reactors

Piero Baraldi [a,*], Camilla Battistini [a], Federico Antonello [b], Jacopo Buongiorno [c], Enrico Zio [a,d]

[a] Energy Department, Politecnico di Milano, Italy
[b] European Space Operation Center, European Space Agency, Germany
[c] Department of Nuclear Science and Engineering, Massachusetts Institute of Technology, Cambridge, MA, United Kingdom
[d] Mines Paris PSL University, France

ARTICLE INFO

*Keywords:*
Nuclear microreactor
Safety analysis
Loss of Heat Sink scenario
Surrogate model
Physics-Informed Neural Network
Allocation points

ABSTRACT

This work explores the development of surrogate models for estimating the evolution of quantities of interest during nuclear reactor accident scenarios. Physics-Informed Neural Networks (PINNs) offer a promising surrogate modelling approach because they allow integrating laws of physics and domain knowledge into traditional Neural Network (NN) surrogates. Specifically, the proposed solution incorporates an additional term in the PINN loss function to enforce physics-based constraints in correspondence of allocation points, which are randomly sampled points whose corresponding target output is not known. As a result, accuracy of the estimation of the quantities of interest and their adherence to the laws of physics are improved. Applications to a synthetic case study and to the response of a nuclear microreactor system during a Loss of Heat Sink scenario confirm that the developed surrogate model based on PINN with allocation points improves the estimation accuracy with respect to other state-of-the-art methods.

List of Acronyms

| Acronym | Full name | Acronym | Full Name | Acronym | Full name |
|---|---|---|---|---|---|
| AOO | Anticipated Operational Occurrence | GP | Gaussian Process | PCE | Polynomial Chaos Expansion |
| ATU | Arbitrary Temperature Unit | HS | Heat Structure | PCU | Power Conversion Unit |
| BDB | Beyond Design Basis | IDPSA | Integrated Deterministic Probabilistic Safety Assessment | PDE | Partial Differential Equation |
| BE | Best Estimate | LHS | Latin Hypercube Sampling | PINN | Physics-Informed Neural Network |
| BEPU | Best Estimate Plus Uncertainty | LOCA | Loss Of Coolant Accident | QoI | Quantity of Interest |
| CCS | Canister Containment Subsystem | LOHS | Loss Of Heat Sink | RF | Reactivity Feedback |

(*continued on next column*)

(*continued*)

| | | | | | |
|---|---|---|---|---|---|
| CD | Control Drum | M&S | Modelling and Simulation | RVACS | Reactor Vessel Auxiliary Cooling Subsystem |
| DB | Design Basis | MIT | Massachusetts Institute of Technology | SR | Shutdown Rod |
| DL | Deep Learning | ML | Machine Learning | SVM | Support Vector Machine |
| DNN | Deep Neural Network | MSE | Mean Squared Error | TDV | Time Dependent Volume |
| DSA | Deterministic Safety Assessment | NB | Nuclear Battery | UQ | Uncertainty Quantification |
| FA | Fuel Assembly | NN | Neural Network | | |
| FMM | Finite Mixture Model | NPP | Nuclear Power Plant | | |

* Corresponding author.
*E-mail address:* piero.baraldi@polimi.it (P. Baraldi).

https://doi.org/10.1016/j.pnucene.2025.105745
Received 23 May 2024; Received in revised form 22 January 2025; Accepted 11 March 2025
Available online 17 March 2025

List of Symbols

| Symbol | Meaning | Symbol | Meaning | Symbol | Meaning |
|---|---|---|---|---|---|
| $D_{BE}$ | Dataset of the accident scenarios simulated using the BE model | $\overline{\overline{Y}}^{(k)}$ | Matrix containing the evolution of the signals in the $k$-th simulated accident scenario | $Loss_{NN}$ | Data fidelity term of $Loss_{PINN}$ (analogous to the loss function of a traditional NN) |
| $N$ | Number of simulated accident scenarios | $P$ | Number of signals simulated by the BE model | $Loss_{phy}$ | Term of $Loss_{PINN}$ that considers the laws of physics |
| $\overline{x}^{(k)}$ | Vector of the parameters describing the conditions of the reactor when the $k-$th simulated accident scenario begins | $\overline{y}_t^{(k)}$ | Vector of the values of the simulated signals at time $t$ in the $k$-th simulated accident scenario | $Loss_{bc}$ | Term of $Loss_{PINN}$ that considers the boundary conditions |
| $d$ | Number of parameters in the vector $\overline{x}^{(k)}$ | $y_{t,i}$ | $i$-th output signal at time $t$ calculated by the BE code | $Loss_{ap}$ | Term of $Loss_{PINN}$ that considers the anchor points |
| $x_i^{(k)}$ | $i$-th parameter of $\overline{x}^{(k)}$ | $D_{SUR}$ | Dataset of the input-output patterns used to train the surrogate model | | |
| $f_{x_i}(\bullet)$ | Probability density function of $x_i$ | $Loss_{PINN}$ | Loss function of the PINN | | |

## 1. Introduction

The safety analysis of nuclear reactors systems requires analyzing the system response during accident scenarios and estimating scenario outcomes (Radaideh and Tomasz, 2020). Modelling and Simulation (M&S) can provide support to gain quantitative and qualitative insights on system safety, in terms of failure probabilities, safety margins and potential outcomes of accident scenarios (Liu et al., 2023). For example, M&S can be used to investigate the behavior of nuclear fuel under normal and abnormal conditions (Stan, 2009), optimize reactor core design (Betzler et al., 2017), assess the response of nuclear systems to transient scenarios such as Loss of Heat Sink (LOHS) accidents (El-Khatib et al., 2013) and Loss of Coolant accidents (LOCA) (Ghosh and Saha, 2021), and quantify key Quantities of Interest (QoI) such as peak temperature values reached during a transient and the related safety margins (D'Auria et al., 2012). The safety analysis can be performed using Best Estimate (BE) M&S tools based on design specifications and physical laws (Avramova and Ivanov, 2010). Indeed, BE models and simulation codes have been used for Deterministic Safety Analysis (DSA) of nuclear reactor systems under the conditions of postulated accident scenarios initiated by Anticipated Operational Occurrence (AOO) events, Design Basis (DB) events and Beyond-Design Basis (BDB) events (D'Auria et al., 2009). Integrated Deterministic and Probabilistic Safety Assessment (IDPSA) (Di Maio et al., 2015) (Unal et al., 2011) and Best Estimate Plus Uncertainty (BEPU) (D'Auria et al., 2012) frameworks have also been proposed to analyze critical scenarios under credible assumptions, considering parameter uncertainty and event occurrence probabilities for providing probabilistic estimates of QoI and safety margins (Zio et al., 2010). However, running many BE code simulations for accurate and statistically robust probabilistic estimates can be computationally prohibitive. Statistics-based frameworks have been introduced, e.g. based on the use of Wilk's theorem (Zio et al., 2010) (Secchi et al., 2008), albeit providing over-conservative estimates and sacrificing information about the full distribution of the QoI (Di Maio et al., 2015).

Surrogate models also have been proposed to obtain fast approximations of the solutions of the original detailed simulation model (Qian et al., 2005) (Tripathy and Bilionis, 2018). The use of these surrogate models in substitution of the computationally intensive detailed models allows the repetition of large number of calculations needed to obtain a significant statistical sample for estimating the probability distributions of QoI (Maulik et al., 2020) and perform sensitivity analyses on the parameters (Ebiwonjumi et al., 2020). Surrogate models are being proposed for use in various applications of engineering (Alizadeh et al., 2020), including in the nuclear field, e.g., to assess the failure probability of passive safety systems (Pedroni and Zio, 2017), to explain the variability of the maximum fuel centerlines and surface temperatures (Radaideh and Tomasz, 2020) and to develop fully autonomous reactor control (Dave et al., 2020). They can be classified into two main categories: reduced order models (ROM) and data-driven models (Benner et al., 2015). ROM are code-intrusive methods aiming at representing a complex system with a reduced number of degrees of freedom, leveraging techniques like proper orthogonal decomposition (POD) (Kang et al., 2022) and reduced basis method (RBM) (Peterson, 1989). Their accuracy relies on the fidelity of the underlying system assumptions and their construction can be challenging when dealing with highly complex and nonlinear systems (Chaturantabut and Sorensen, 2010). On the other hand, data-driven surrogate models generalize the input/output physical relationships by creating a mathematical representation of the original model based on samples of input/output data (Worrell et al., 2019; Herman et al., 2020). Data-driven models rely on Machine Learning (ML) and Deep Learning (DL) algorithms for parameters calibration. Examples of ML methods are Polynomial Chaos Expansion (PCE) (Ebiwonjumi et al., 2021), Support Vector Machines (SVM) (Zio et al., Failure and reliability prediction by support vector machines regression of time series data 2011) (Hurtado, 2007), Finite Mixture Models (FMM) (Puppo et al., 2021), Gaussian Processes (GP) (Yurko et al., 2015) (Yoon et al., 2021) and Artificial Neural Networks (ANN) (Baraldi et al., 2012) (Lek and Park, 2008). Some ML methods encounter challenges in managing intricate and unstructured data patterns (Dargan et al., 2020). Recently, Deep Learning (DL) methods, such as Deep Gaussian Processes (Damianou and Neil, 2012) and Deep Neural Networks (Conner et al., 2021) have exhibited significant capabilities in learning intricate patterns from large datasets, allowing reconstructing long transients and improving accuracy and scalability (Price et al., 2022).

When developing data-driven surrogate models to substitute BE models in safety analysis, the following objectives are typically considered: *i*) accuracy, which quantifies how close is the estimation of the QoI provided by the surrogate model to that provided by the BE model, *ii*) computational efficiency, i.e. the reduction of the computational burden achieved by using a surrogate model instead of the BE model. Two additional objectives are: *iii*) consistency of the estimates provided by the surrogate model with the laws of physics governing the system behavior, to enhance the trustworthiness of the surrogate model, especially when used in regions not well covered by the training patterns, *iv*) capability of dealing with the complex dynamics of system response to operational and incidental transients (Wu and Kozlowski, 2017), and particularly providing accurate estimates of the QoI in those parts of the transients which are of most interest for the safety analysis. Actually, traditional approaches to the development of surrogate models for the safety analysis of nuclear reactors focus mainly on the objectives of accuracy and computational efficiency (*i*) and *ii*), above) (Arrieta et al., 2020)(Radaideh and Tomasz, 2020). A surrogate model based on Physics-Informed Neural Networks (PINNs) has been developed in (Antonello et al., 2023b) to obtain accurate, computationally efficient

and physics-consistent (objective *iii*), above) estimates of specific QoI. The physics consistency has been embedded into the PINNs by introducing in the loss function for the training of the model a term that evaluates the mismatch between the estimates and the laws of physics (Raissi et al., 2019).

In this work, we consider the problem of obtaining accurate estimates of safety-relevant QoI in specific time intervals of transients developing in a nuclear reactor (objective *iv*), above). Examples are the peak temperature reached during a transient process for Peak Shaving scenario (Yang et al., 2023), temperature impulses resulting from some critical event occurrence (Vedros et al., 2022), pressure, temperature and stress of cladding under accident conditions (Hózer et al., 2023). Quantities such as those mentioned are crucial for safety analysis as they are representative of system behavior at the onset, aftermath and critical instances of a transient on accident (Ryu et al., 2022).

For the estimation of the QoI, in this work we use a surrogate model based on PINNs, whose loss function for training contains also a term computed in correspondence of allocation points (Wuest et al., 2016). These are randomly sampled points in the multi-dimensional input space, at which the verification of the laws of physics is reinforced by evaluating the consistency of the corresponding PINNs output with the law of physics. Note that the allocation points physics-consistency verification avoids using the computationally heavy BE models to obtain additional input\output data.

The main contributions of this work are:

- the definition of a new loss function for the training of PINNs that, by using allocation points, allows obtaining accurate estimates of the QoI in specific time intervals, without requiring to perform additional simulations with the BE model;
- the comparison of the performance of the developed PINNs-based surrogate model with other state-of-the-art approaches, considering the error in the estimates of the QoI during critical time intervals.

The effectiveness of the proposed approach is tested by application to a synthetic simulation scenario and a BE model of the Loss of Heat Sink (LOHS) accident in a Nuclear Battery (NB), which is a class of transportable, plug-and-play, nuclear microreactors (Buongiorno et al., 2021).

The remainder of the paper is organized as follows: Section 2 presents the case-study of the NB; Section 3 describes the developed PINNs with allocation points; Section 4 shows the results on two case studies; Section 5 draws the conclusions and highlights potential future developments.

## 2. Nuclear battery case study

Nuclear Batteries (NBs) are standardized micro-reactors built to generate 1–20 MW of low-carbon energy suitable for various applications, such as chemical processes, water desalination and hydrogen production (Buongiorno et al., 2021). The focus of the present work is on a 5 MW high-temperature heat pipe reactor developed at the Massachusetts Institute of Technology (MIT) (Buongiorno et al., 2021). The reactor is composed of solid graphite blocks featuring channels that accommodate neutron moderators, fuel elements and heat pipes. The core is enclosed in a Canister Containment Subsystem (CCS), which in an emergency can be cooled by a Reactor Vessel Auxiliary Cooling Subsystem (RVACS) that removes the residual heat. Shutdown Rods (SRs) enable quick shutdowns, while during normal operation the heat pipes efficiently transfer heat to a Power Conversion Unit (PCU) for semi-autonomous operations.

The present work considers the unprotected Loss of Heat Sink (LOHS) accident scenario (Feldman et al., 1987), where the PCU suddenly loses its ability to transfer the heat from the secondary side, and in addition it is postulated neither the Control Drums (CDs) nor the SRs are actuated, thus relying solely on Reactivity Feedback (RF) and radial heat removal through the core via conduction, ultimately reaching the RVACS for dissipation.

**Table 1**
Input of the BE model, i.e. the parameters used to describe the reactor conditions when the LOHS accident scenario begins and corresponding probability distributions.

| Symbol | Notation | Parameter | Probability distribution | Nominal Value [range][distribution] |
|---|---|---|---|---|
| $P_{NB}$ | $x_1$ | NB power | Uniform | $5MW$ $[\mp 15\%]$ |
| $\alpha$ | $x_2$ | Fuel reactivity feedback coefficient | Uniform | $-\frac{1.5pcm}{K}[\mp 15\%]$ |
| $K_g$ | $x_3$ | Graphite thermal conductivity | Uniform | Function dependent on Graphite Temperature whose coefficient varies within $[\mp 10\%]$ of its nominal value |
| $GC_{fc}$ | $x_4$ | Gap conductance between fuel and cladding | LogUniform | $10^4$ W/ $m^2$-K $[5 \times 10^3 - 10^5]$ |
| $GC_{fa}$ | $x_5$ | Gap conductance between adjacent fuel assemblies | LogUniform | $10^4$ W/ $m^2$-K $[5 \times 10^3 - 10^5]$ |
| $GC_{cg}$ | $x_6$ | Gap conductance between cladding and graphite | LogUniform | $10^4$ W/ $m^2$-K $[5 \times 10^3 - 10^5]$ |
| $GC_{NB}$ | $x_7$ | Gap conductance between canister and reflector | Uniform | 70 W/ $m^2$-K $[40 - 120]$ |
| $A_R$ | $x_8$ | RVACS flow area | Uniform | $0.3\ m$ $[0.2 - 0.4]$ |
| $T_R$ | $x_9$ | RVACS input air temperature | Uniform | $300\ K$ $[270 - 320]$ |
| $k_R$ | $x_{10}$ | RVACS wall roughness | LogUniform | $10^4$ $[10^3 - 10^5]$ |

### 2.1. The BE model for the LOHS accident scenario

The simulation of the LOHS accident scenario is performed based on a BE model developed using RELAP3D-5 (Antonello et al., 2023a). The model represents the NB with Heat Structures (HS), to mimic system components, and gap conductance to represent heat transfer between these structures. The loss of the secondary system is simulated as an adiabatic boundary condition for the heat pipes, consequently heat transfer is redirected to the RVACS, which is modeled as a pipe element based on Time-Dependent Volumes (TDV) to simulate the air source and sink.

Table 1 reports the list of parameters that define the conditions of the reactor when the accident scenario begins. Specifically, the vector $\overline{x}^{(k)} = \left[x_1^{(k)}, x_2^{(k)}, \ldots, x_d^{(k)}\right] \in R^d$ with $d = 10$, contains the values of the 10 parameters at the beginning of the $k$-th simulated LOHS accident. The uncertainty in the values of these parameters is represented using the probability density functions $f_{x_i}(\bullet)$, $i = 1, \ldots d$, reported in the last column of Table 1, taken from (Antonello et al., 2023a).

Given the initial condition $\overline{x}^{(k)}$, the BE model simulates the unprotected LOHS considering the following phases: 1) an initial period of time during which the reactor is in normal operation condition, 2) the sudden loss of heat transfer from the heat pipes to the heat sink and 3) the evolution of the transient for 350 time steps, where each time step corresponds to 10 s. The output of the BE model for a given input vector is a $P$-dimensional time series $\overline{\overline{Y}}^k = \left[y_t\right]_{t=0}^{T} \in R^{P \times T}$, with $T$ indicating the time interval between the beginning of the LOHS scenario and the end of

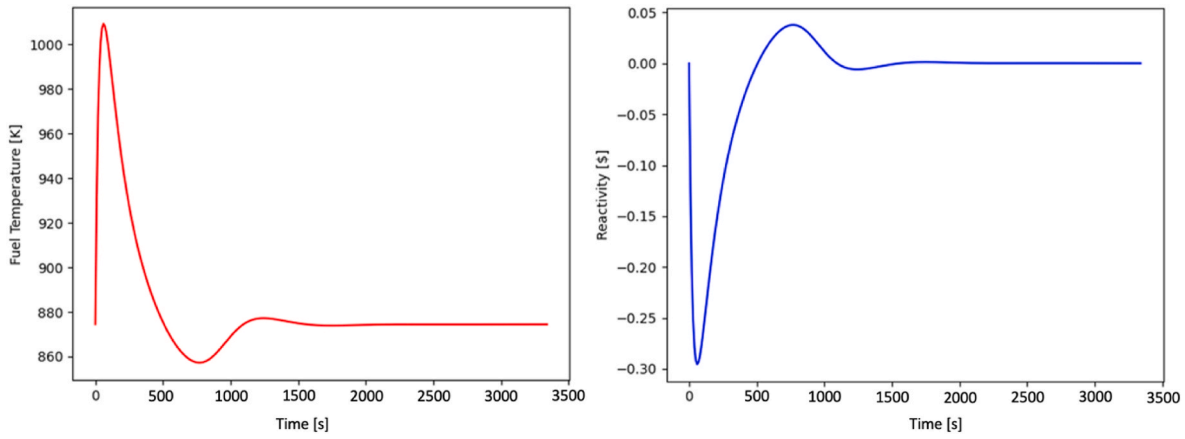


**Fig. 1.** Fuel temperature and reactivity evolution during a LOHS accident scenario simulated by the BE code.

the convergence of the accident scenario towards a stable state, which has been found to be always before $T = 1500$ seconds. Among the $P > 1000$ parameters modeled by the BE, some examples are the fuel average temperature $(T_f)$, in the hot Fuel Assemblies (FA), the net reactivity $(\rho)$, the peak cladding temperature $(T_c)$ and the RVACS heat removal rate $(P_R)$. The vector $\overline{Y}_t = \left[y_{t,i}\right]_{i=1}^{P} \in R^P$ contains the values $y_{t,i}$ of signal $y_i$ at time $t$. Fig. 1 shows an example of the evolution of the fuel temperature in the hot FA and of the reactivity during the first 3500 s of a transient. The temperature increases following the occurrence of the LOHS and reaches its maximum value after 50 s. The increase of the temperature leads the RF to shut down the NB by decreasing the reactivity.

## 3. The surrogate model

Section 3.1 describes the data and physics-based knowledge used to develop the surrogate model based on PINNs. Section 3.2 discusses the structure of the PINN model in terms of input and output quantities. Section 3.3 presents the novel approach developed in this work for the physics-informed training of the PINN surrogate model with allocation points.

### 3.1. Data and physics-based knowledge used to develop the surrogate model

The PINN surrogate model is developed using data simulated by the BE model described in Section 2.1 and physics-based knowledge about the neutronics in the reactor.

With regard to the data, the BE model is used to build a dataset, $D_{BE} = \left\{\left(\overline{x}^{(k)}, \overline{\overline{Y}}^{k}\right)\right\}_{k=1}^{N}$, containing $N$ input\output patterns, each one representing the system response to a LOHS accident scenario. The generic $k$-th pattern is made by the vector of parameter values $\overline{x}^{(k)}$ representing the conditions of the reactor when the $k$-th simulated LOHS accident scenario initiates and the multidimensional time series $\overline{\overline{Y}}^{(k)}$ of the system response signals evolution during the scenario. The pattern $\left(\overline{x}^{(k)}, \overline{\overline{Y}}^{(k)}\right)$ is generated by:

- sampling the values of the parameters $\left[x_1^{(k)}, x_2^{(k)} \ldots, x_d^{(k)}\right] \in R^d$ from the corresponding probability distributions $f_{x_i}(\bullet)$ using the Latin-Hypercube sampling (LHS) technique (Mckay et al., 1979);
- running the BE code to simulate the time evolution of the $P$ system response signals $\overline{\overline{Y}}^{(k)}$.

Note that the number of LOHS accident scenarios that can be simulated is typically limited by the large computational cost required for performing the BE simulation. Specifically, in this work $N = 250$ accident scenarios have been simulated with the BE model of Section 2.2.

With regard to the physics-based knowledge, the reactivity feedback equation (Henry, 1958):

$$\frac{\partial \rho}{\partial t} + \alpha \frac{\partial T_f}{\partial t} = 0 \tag{1}$$

and the initial boundary condition:

$$\rho(0) = 0 \tag{2}$$

are considered. Equation (1) provides a simplified representation of the time-dependent behavior of the reactivity feedback in response to fuel temperature changes during a transient, where the reactivity coefficient $\alpha$ describes the variation of reactivity corresponding to the variation of $1K$ of the average fuel temperature. The equation considers only the variation of reactivity due to temperature variations, whereas it ignores other effects and the reactivity control via CDs and SRs.

### 3.2. Input and output of the surrogate model

In this work, the surrogate model receives as input the vector $\overline{x}$ of the reactor parameters when the accident scenario begins and the time $t$ at which we want to estimate the output signals $y_1$ (average fuel temperature) and $y_2$ (reactivity). Note that the surrogate model estimates only two QoI among the $P > 1000$ signals provided by the BE model. Specifically, the average fuel temperature is one of the most critical QoI directly connected with the reactor safety limits (Antonello et al., 2023b) and the reactivity is used for the verification of the consistency of the estimates with Equation (1).

The choice of feeding the time $t$ as input to the surrogate model allows reducing the complexity of the problem with respect to estimating the entire multidimensional time series $\overline{\overline{Y}}$ from the input $\overline{x}$. Specifically, the surrogate model provides the mapping $[\overline{x}, t] \longrightarrow \overline{y}_t$ from $R^{d+1}$ to $R^2$, whereas estimating the entire time series would require mapping $[\overline{x}] \longrightarrow \overline{\overline{Y}}$ from $R^d$ to $R^{2\times T}$, which is significantly more complex particularly when long transients are considered.

### 3.3. PINNs with allocation points

The surrogate model developed in this work is based on the use a new type of PINNs. Traditional PINNs incorporate the physics knowledge described by equations governing the system, typically in the form of Partial Differential Equations (PDEs) and Boundary Conditions (BCs). This is obtained by adding physics-based terms, $Loss_{phy}$ and $Loss_{bc}$, to the

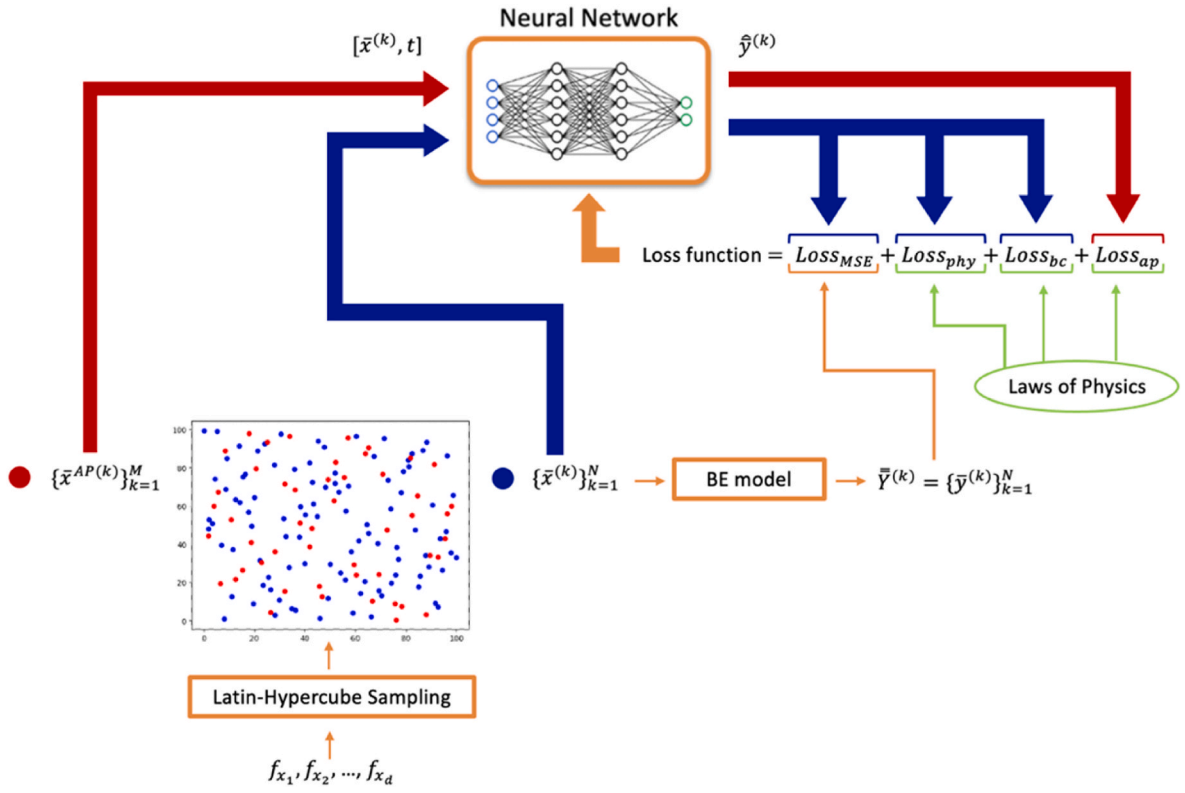


**Fig. 2.** Schematic representation of PINNs with allocation points.

loss function of a NN, $Loss_{NN}$ considered for its training (Raissi et al., 2019):

$$Loss_{PINN} = Loss_{NN} + Loss_{phy} + Loss_{bc} \tag{3}$$

In this work, $Loss_{NN}$ is the mean squared error between the signal estimates $\hat{\bar{y}}_t^{(k)}$ provided in output by the surrogate model and the output results of the BE code $\bar{y}_t^{(k)}$, computed over the training set of input/output patterns:

$$Loss_{NN} = \frac{\sum_{(k,t)}^{(N,T)} \left(\bar{y}_t^{(k)} - \hat{\bar{y}}_t^{(k)}\right)^2}{N \bullet T} \tag{4}$$

The loss terms $Loss_{phy}$ and $Loss_{bc}$ are introduced to ensure coherence of the PINN output with the governing laws of physics and the boundary conditions of the physical problem, respectively. The computation of these terms requires generating the training dataset $D_{SUR} = \left\{\left(\bar{x}^{(k)}, t\right), \bar{Y}_t^{(k)}\right\}_{k=1\ldots N, t=0\ldots T}$ of $N \bullet T$ input $\left(\bar{x}^{(k)}, t\right)$/output $\left(\bar{y}_t^{(k)}\right)$ patterns, from the dataset $D_{BE} = \left\{\left(\bar{x}^{(k)}, \bar{\bar{Y}}^{(k)}\right)\right\}_{k=1}^{N}$ of the accident simulations.

Concerning the physics-based term of the loss function, $Loss_{phy}$, it leverages the knowledge of the RF equation (Equation (1)), which is rewritten as:

$$\frac{\partial y_2}{\partial t} + x_2 \frac{\partial y_1}{\partial t} = 0 \tag{5}$$

Specifically, $Loss_{phy}$ measures the inconsistency of the PINN estimates with the equation and it is computed as:

$$Loss_{phy} = \frac{\sum_{(k,t)}^{(N,T)} \left(\frac{\partial \hat{y}_{2,t}^{(k)}}{\partial t} + x_{2,t}^{(k)} \frac{\partial \hat{y}_{1,t}^{(k)}}{\partial t}\right)^2}{N \bullet T} \tag{6}$$

$Loss_{bc}$ considers the constraint imposed by the boundary conditions of the accident scenario (Equation (2)), which can be rewritten as:

$$y_{2,0} = 0 \tag{7}$$

and it is computed as:

$$Loss_{bc} = \frac{\sum_{k=1}^{N} \left(y_{2,0}^{(k)} - \hat{y}_{2,0}^{(k)}\right)^2}{N} \tag{8}$$

The accuracy of the estimates provided by the PINN is strongly affected by the number of input/output patterns available for training. In this work, the large computational burden for performing a single simulation with the BE code (Memmott et al., 2010), makes it impractical to generate a large number of input/output patterns for the minimization of $Loss_{PINN}$ during the PINN training. For this reason, we introduce an additional term in the loss function, drawing from the work of (Mathias et al., 2022) in the different context of solving PDEs. The idea is to quantify how well the PINN output is consistent with the physics-based knowledge on a set of accident scenarios different from those used to compute the other terms of the loss function. Specifically, at each iteration of the PINN training (epoch), $M$ vectors of input parameters of the accident scenarios $\bar{x}^{AP(k)}$, $k = 1, \ldots, M$, hereafter referred to as Allocation Points (AP), are randomly sampled from their probability density functions $f_{x_i}(\bullet)$ using the LHS technique, and the PINN output values $\hat{\bar{y}}_t^{AP(k)}$ are computed from the $M \bullet T$ input parameters values $\left(\bar{x}^{AP(k)}, t\right)$ for $k = 1, \ldots, M$ and $t = 0, \ldots, T$. The new 'consistency' term of the loss function can, then, be computed as:

$$Loss_{ap} = \frac{\sum_{(k,t)}^{(M,T)} \left(\frac{\partial \hat{y}_{2,t}^{AP(k)}}{\partial t} + x_{2,i} \frac{\partial \hat{y}_{1,t}^{AP(k)}}{\partial t}\right)^2}{M \bullet T} \tag{9}$$

Note that the computation of this new term of the loss function does not require additional runs of the BE code. Also, the use of different allocation points in the different epochs provides robustness and ensures

the capability of generalization of the surrogate model. The total loss function $Loss_{TOT}$, for the training of the PINN with allocation points is, then:

$$Loss_{TOT} = Loss_{MSE} + Loss_{phy} + Loss_{bc} + Loss_{ap} \quad (10)$$

The overall training procedure is summarized in Fig. 2.

## 4. Results

The proposed approach is evaluated considering two case studies:

1. A synthetic case study in which simplified analytical functions are used to simulate signals like if they were measured in accident scenarios. This allows a controlled preliminary assessment of the effectiveness of the proposed approach.
2. The nuclear battery case study detailed in Section 2.

The performance of the proposed approach is compared with that of NNs and PINNs (without allocation points). In both case studies, the performance metrics are computed by considering a set of $N^{test}$ accident scenarios simulated using the simplified analytical functions in the synthetic case study and the BE code in the nuclear battery case study. These accident scenarios are different from those used to train the models. The following metrics are considered for the comparison:

- the mean error of estimation of signal $y_1$ on the entire $k$-th accident scenario, which will be referred to as global error on the $k$-th accident scenario ($Err_{glo}^{(k)}$). It is computed as the Root Mean Squared Error (RMSE) between the signal value $y_{1,t}^{(k)}$ (simulated using the simplified analytical functions in the synthetic case study and the BE code in the nuclear battery case study) and the corresponding estimate provided by the surrogate model $\hat{y}_{1,t}^{(k)}$:

$$Err_{glo}^{(k)} = \sqrt{\frac{\sum_{t=1}^{T}\left(y_{1,t}^{(k)} - \hat{y}_{1,t}^{(k)}\right)^2}{T}} \quad (11)$$

- the mean error of estimation of signal $y_1$ on all accident scenarios:

$$Err_{glo} = \sqrt{\frac{\sum_{k=1}^{N^{test}}\left(Err_{glo}^{(k)}\right)^2}{N^{test}}} = \sqrt{\frac{\sum_{(k,t)=(1,1)}^{(N^{test},T)}\left(y_{1,t}^{(k)} - \hat{y}_{1,t}^{(k)}\right)^2}{N^{test} \bullet T}} \quad (12)$$

- the mean error of estimation of the QoI in a defined time interval of the accident scenario, e.g. signal $y_1$ in the initial part, at the end or near the peak, which will be referred to as local error ($Err_{loc}$). Given a small time interval of interest $[t^* - \Delta, t^* + \Delta]$, the error metric is computed as:

$$Err_{loc} = \sqrt{\frac{\sum_{k=1}^{N^{test}}\sum_{t\in[t^*-\Delta,t^*+\Delta]}\left(y_{1,t^*}^{(k)} - \hat{y}_{1,t^*}^{(k)}\right)^2}{N^{test} \bullet N^{\Delta T}}} \quad (13)$$

where $N^{\Delta T}$ is the number of simulated time instants in the interval $[t^* - \Delta, t^* + \Delta]$.

Following the procedure proposed in (Antonello et al., 2023b), 250 accident scenarios are simulated for both case studies. A dataset $D_{BE} = \left\{\left(\bar{x}^{(k)}, \bar{\bar{Y}}^{k}\right)\right\}_{k=1}^{180}$ of $N = 180$ of these accident scenarios is used for training the NN and PINN surrogate models (training set), 30 accident scenarios (validation set) are used for setting the hyperparameters, and 40 accident scenarios (test set) are used for evaluating their performances by computing the metrics of Equations (12) and (13). An additional set $\left\{\bar{x}^{AP(k)}\right\}_{k=1}^{M}$ of $M = 180$ allocation points sampled from the probability distributions $f_{x_i}(\bullet)$ is used for the training of the PINN with AP. The results of the application of the proposed approach to the synthetic and nuclear battery case studies are presented in Sections 4.1 and 4.2, respectively.

**Table 2**
Synthetic case study: parameters of the model, physics-based interpretation and probability distributions.

| Parameter | Physics-related meaning | Type of probability distribution | $[min, max]$ in AU |
|---|---|---|---|
| $x_1$ | Amplitude of the oscillations of $y_1$ and $y_2$ | Uniform | $[100, 200]$ |
| $x_2$ | Parameter related to the peak value of $y_1$ and $y_2$ | Uniform | $[0.05, 0.25]$ |
| $x_3$ | Parameter related to the period of the oscillations of $y_1$ and $y_2$ | Uniform | $[0.8, 1.2]$ |
| $x_4$ | Initial value of $y_1$ | Uniform | $[800, 900]$ |
| $x_5$ | Coefficient of proportionality between $y_1$ and $y_2$ | Uniform | $[0.001, 0.005]$ |

**Table 3**
Synthetic case study: architecture and hyperparameters of the underlying surrogate model.

| Number of hidden layers | Number of neurons per layer | Activation function | Activation function parameter | Number of epochs |
|---|---|---|---|---|
| 2 | $6, 256, 128, 2$ | Exponential Linear Unit ($ELU$) | $\alpha = 1$ | 100000 |

### 4.1. Synthetic case study

The synthetic dataset is generated using analytic functions in a way to somehow mimic the input/output relationships of the BE model. Specifically, we consider a 5-dimensional vector, $\bar{x} \in R^5$, and a 2-dimensional vector, $\bar{y} \in R^2$, related according to the model:

$$y_{1,t} = x_4 + x_1(1 - x_2 t)sin(x_3 t)\ y_{2,t} = x_5 x_1(x_2 t - 1)sin(x_3 t) \quad (14)$$

with the initial condition $y_{2,0} = 0$.

Table 2 reports the probability distributions from which the vectors $\bar{x}^{(k)}$ are sampled to generate the training, validation and test sets. As the governing equations are not derived from physical laws, input and output quantities are expressed in Arbitrary Units (AU).

As done in Section 3.1 for the simulation of the LOHS accident scenarios in NBs, we assume the availability of the differential equation:

$$\frac{\partial y_2}{\partial t} + x_5\frac{\partial y_1}{\partial t} = 0 \quad (15)$$

which mimics a law of physics and it is fully satisfied by the equations used to simulate the data. Table 3 reports the architecture of the developed surrogate model. For fairness of comparison, NN, PINN and PINN with AP are developed using the same underlying architecture, which has been set by trial-and-error considering the performance on the validation set. The first layer of the three models has six neurons, corresponding to the six input signals, $x_1, x_2, \ldots, x_5$ and the time $t$, as shown in Fig. 2.

To account for the variability of the training process, which depends also on the initialization of the NN weights, the training of the model is repeated 10 times, each time using a different random initialization.

Three small time intervals are considered for the computation of the

**Table 4**
Synthetic case study: performances of the proposed and comparison surrogate models. Loc1 refers to the first 5 points, Loc2 to the 5 points around the peak and Loc3 to the last 5 points of the accident scenarios. The last column reports a measure of coherence between the estimates and Equation (14), which is computed applying the physic-based term of the loss function $Loss_{phy}$ to the test set.

| | $Err_{glo}$ in AU | $Err_{loc,1}$ in AU | $Err_{loc,2}$ in AU | $Err_{loc,3}$ in AU | Accordance with physics (measured through law of physics) |
|---|---|---|---|---|---|
| PINN with AP (Proposed approach) | 0.53 | 0.39 | 0.49 | 0.69 | $2.60 \times 10^{-7}$ |
| PINN | 0.74 | 0.48 | 0.36 | 1.25 | $5.04 \times 10^{-6}$ |
| NN | 0.83 | 0.47 | 0.55 | 1.49 | $7.49 \times 10^{-5}$ |

metrics $Err_{loc}$ related to the local accuracy in correspondence of QoI:

- the first five points of the accident scenario ($Err_{loc,1}$);
- an interval of five points centered on the peak of $y_1$ ($Err_{loc,2}$);
- the last five points of the accident scenario ($Err_{loc,3}$).

Table 4 reports the performances of the proposed PINN with AP surrogate model and of those considered for comparison (NN, PINN) in terms of global and local metrics computed on the test set. The reported values refer to the average of the global accuracy $Err_{glo}$ from 10 runs of the surrogate models trained using 10 different initializations of the weights.

With regard to the global accuracy, the developed surrogate model is significantly more accurate than the NN and PINN considered for comparison, with a reduction of 36% of the error with respect to the NN and of 28% with respect to the PINN. Note that in two cases out of three the proposed PINN model with AP outperforms NN and PINN when local accuracy metrics are considered. With regard to the peaks, it should be observed that all models provide relatively small errors if compared with the average error over the whole accident scenario, although PINN provides the most accurate estimates. The last column of Table 4 reports a measure of the accordance of the estimates with Equation (15). As expected, the PINN with AP provides the estimates most in agreement with the physics law, which confirms the opportunity of adding the loss term $Loss_{ap}$ to the total loss function used to train the surrogate model.

Fig. 3 illustrates two representative examples of application to accident scenarios of the proposed approach and comparison approach. The graphs at the top show the evolution of signal $y_1$, simulated using Equation (14), whereas the graphs at the bottom show the corresponding estimation errors (pointwise differences between the simulated trajectory and the estimates). Notably, PINN with AP tends to exhibit errors smaller than 1, whereas traditional NN and PINN show larger errors in specific time intervals, particularly at times greater than 5 s.

It is also interesting to observe that all three surrogate models give the largest error on the same accident scenario (Fig. 4), which is characterized by a relatively high positive peak of $y_1$. Specifically, the mean error of estimation of the average fuel temperature on this entire accident scenario ($Err_{glo}^{(k)}$ in eq. (11)) for the NN is 2.61 AU, for the PINN is 2.26 AU and for the PINN with AP is 1.21 AU. This shows that the introduction of the physics-based information in the PINN surrogate

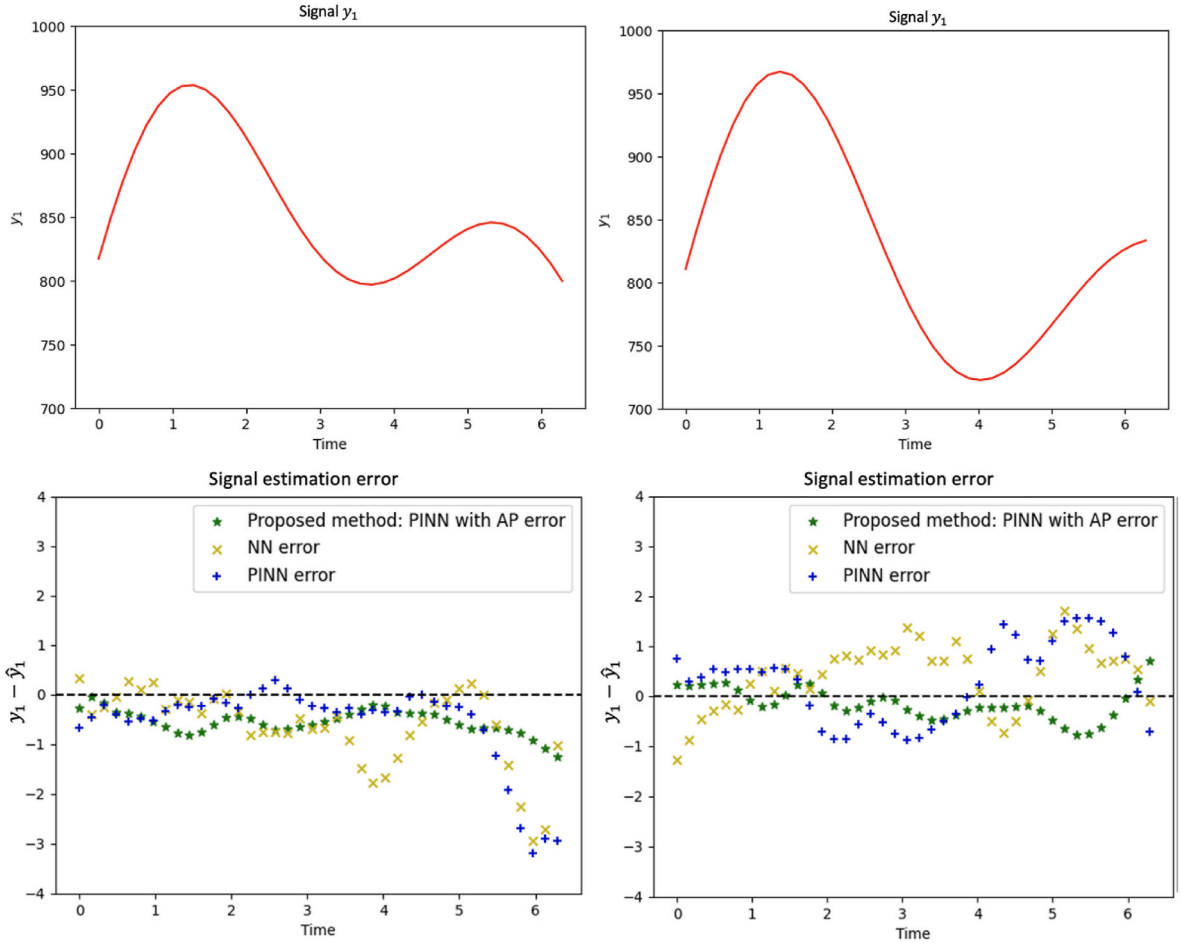


**Fig. 3.** Synthetic case study: $y_1$ (top) and estimation error (bottom) in two representative accident scenarios.

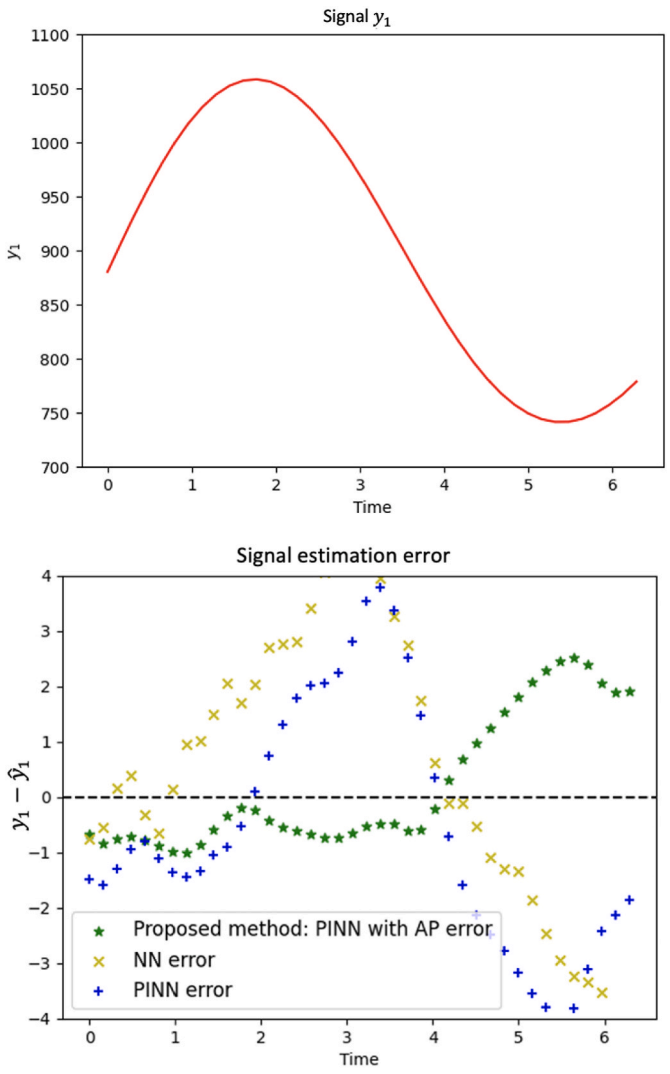


**Fig. 4.** Synthetic case study: $y_1$ (top) and estimation error (bottom) for the accident with the largest global estimation error.

**Table 5**
Architecture and hyperparameters.

| Number of hidden layers | Number of neurons per layer | Activation function | Activation function parameter | Number of epochs |
|---|---|---|---|---|
| 6 | 11, 128, 64, 32, 32, 16, 4, 2 | Exponential Linear Unit (*ELU*) | $\alpha = 128, 64, 32, 32, 16, 4$ | 2000 |

model with AP significantly reduces the error, particularly between time 2 and 4 where the signal derivative is steepest. Within the time interval between 4 and 6, which corresponds to the negative peak of the signal, all approaches exhibit relatively large absolute errors. However, the PINN with AP underestimates the signal value (positive error), whereas the other models overestimate it (negative error). This discrepancy arises from the tendency of traditional NN approaches of smoothing both positive and negative peaks. In contrast, PINN with AP is seen to effectively capture the signal dynamics in correspondence of the positive peak, at the cost of amplifying the negative peak. Future work will investigate this issue, by running of the automatic generation of APs in critical time intervals.

### 4.2. NB safety analysis with regards to LOHS accident scenarios

Table 5 reports the architecture used for the NN, PINN and PINN with AP developed for the analysis of the LOHS accident scenarios in the NB. Note that the architecture is deeper (6 hidden layers) and with more neurons per layer than the architecture used in the previous synthetic case study (Section 4.1). This is because the input/output relationship for this case study is complex and highly nonlinear, which requires the use of a deeper architecture than for the previous synthetic case study.

Table 6 reports the global and local performance metrics on the test set. The proposed surrogate model allows obtaining a slight improvement on the global accuracy with respect to other state-of-the-art approaches and a more significant improvement of the local accuracy, especially in correspondence of the peak temperature, which is a most critical QoI for the safety analysis of NBs. The improvement of the performance is obtained by driving the training of the model towards solutions more consistent with the physics, as it can be observed in the last column of Table 6.

Fig. 5 shows two examples of estimates of QoIs in LOHS accident scenarios. The PINN with AP tends to significantly outperform the traditional PINN at the end of the accident scenario, where the slope of the signal $y_1$ is small, whereas the improvement of the local accuracy at the beginning of the accident scenario, where the slope is big, is smaller. This difference in the performance may depend on the approximation made by the law of physics (Equation (1)) that does not capture all effects influencing the signal evolution in the initial part of the accident scenario.

These results demonstrate that PINNs with AP provide more accurate and physically consistent estimations of QoIs during nuclear reactor accident scenarios compared to other state-of-the-art surrogate models. This is particularly valuable for safety analysis of nuclear reactors, where relying on computationally prohibitive best-estimate models is impractical.

## 5. Conclusions

Nuclear reactor safety analysis requires estimating the evolution of key QoI for a large number of accident scenarios. However, performing

**Table 6**
NB LOHS case study: performances of the proposed and comparison approaches. Loc,1 refers to the first 5 points, Loc,2 to the 5 points around the peak and Loc,3 to the last 5 points of the accident scenarios. Relative error reductions with respect to the NN model, computed as $(Err^{NN} - Err)/Err^{NN}$, are reported in square brackets. The fifth column presents a measure of coherence between the estimates and Equation (5), computed by applying the physics-based term of the loss function $Loss_{phy}$ to the test set. Relative reductions of $Loss_{phy}$ are reported in square brackets.

| | $Err_{glo}$ $(K)$ [relative error reduction with respect to NN] | $Err_{loc,1}$ $(K)$ [relative error reduction with respect to NN] | $Err_{loc,2}$ $(K)$ [relative error reduction with respect to NN] | $Err_{loc,3}$ $(K)$ [relative error reduction with respect to NN] | Accordance with physics (measured through law of physics) [relative of reduction of $Loss_{phy}$] |
|---|---|---|---|---|---|
| NN | 1.50 | 1.84 | 1.48 | 2.10 | 232468 |
| PINN | 1.31 [12.68%] | 1.99 [− 8.15%] | 1.30 [12.16%] | 1.67 [20.48%] | 2612 [98.87%] |
| PINN with AP (Proposed approach) | 1.26 [16.00%] | 1.32 [28.26%] | 0.98 [33.78%] | 1.62 [22.86%] | 6 [99.99%] |

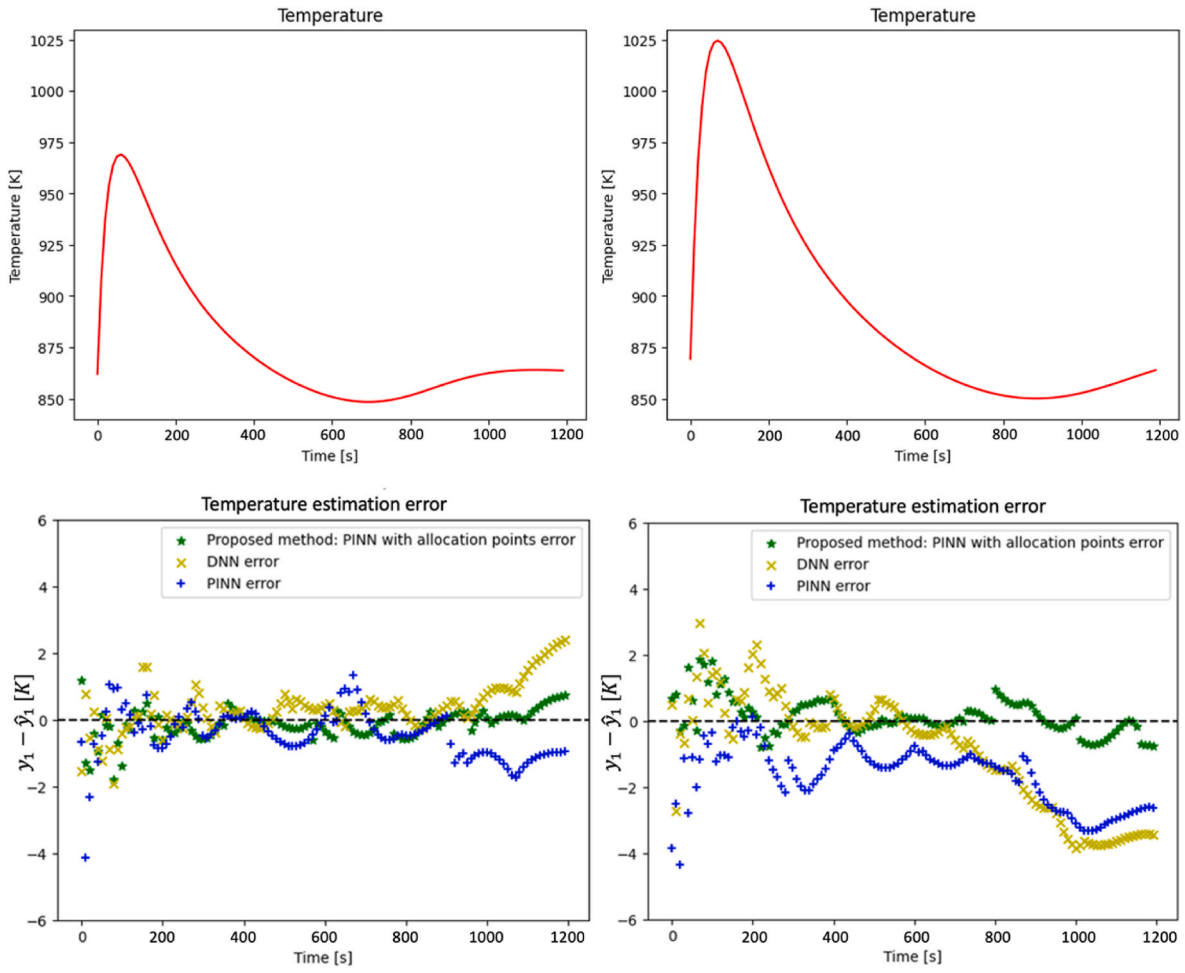


**Fig. 5.** NB LOHS case study: Fuel Temperature (top) and estimation error (bottom) in two accident scenarios.

simulations using computationally expensive BE models for each scenario is often impractical. In the present work, we have proposed a novel approach based on PINNs to develop accurate and computationally efficient surrogate models for the simulation of accident scenarios. By incorporating physical laws into the neural network structure, PINNs can be trained on a limited set of accident scenarios simulated using BE models. Once the PINN-based surrogate model has been trained, it can be used to estimate QoI with affordable computational cost. In order to improve the accuracy of the estimates and further ensure physical consistency of the surrogate model estimates, without having to increase the number of data used for model training to be generated, a new term has been added to the traditional loss function of PINNs to enforce physical consistency. The performance of the proposed approach for surrogate modeling has been compared with that of traditional NNs and PINNs. The results obtained on a synthetic case study and on the analysis of LOHS accident scenarios in a nuclear microreactor system show that: *i*) the global accuracy of the proposed surrogate model is more satisfactory than that of the NN and PINN and *ii*) the estimation of QoI for the safety analysis in critical time intervals is significantly more accurate. The increase of accuracy and consistency of the estimates of QoIs stem from the integration of laws of physics into the loss function minimized during surrogate model training. Given the promising results achieved in estimating QoI for LOHS accidents in nuclear microreactors, future work will focus on demonstrating the effectiveness of the proposed approach for other accident scenarios and reactor types. To further enhance trustworthiness of the use of surrogate models for nuclear reactor safety analysis, they should also be able to quantify uncertainty in the estimates. This is an important direction of future research regarding the use of UQ methods for the estimation of the local errors of the surrogate models. Demonstration of the proposed approach on other accident scenarios and reactor types, and quantification of uncertainty are decisively important for the acceptance of the use of surrogate models in safety-critical nuclear applications.

## CRediT authorship contribution statement

**Piero Baraldi:** Writing – review & editing, Visualization, Validation, Supervision, Resources, Methodology, Formal analysis, Conceptualization. **Camilla Battistini:** Writing – original draft, Visualization, Software, Methodology, Formal analysis, Conceptualization. **Federico Antonello:** Writing – review & editing, Visualization, Software, Methodology, Formal analysis, Conceptualization. **Jacopo Buongiorno:** Writing – review & editing, Supervision, Resources, Project administration, Funding acquisition, Conceptualization. **Enrico Zio:** Writing – review & editing, Supervision, Resources, Project administration, Funding acquisition, Conceptualization.

## Declaration of competing interest

The authors declare the following financial interests/personal relationships which may be considered as potential competing interests: Piero Baraldi reports financial support was provided by FAIR (Future Artificial Intelligence Research). If there are other authors, they declare that they have no known competing financial interests or personal relationships that could have appeared to influence the work reported in this paper.

## Acknowledgment

This work is supported by FAIR (Future Artificial Intelligence Research) project, funded by the NextGenerationEU program within the PNRR-PE-AI scheme (M4C2, Investment 1.3, Line on Artificial Intelligence)

## Data availability

The data that has been used is confidential.

## References

Alizadeh, Reza, Allen, Janet K., Mistree, Farrokh, 2020. Managing computational complexity using surrogate models: a critical review. Res. Eng. Des. 31 (3), 275–298. https://doi.org/10.1007/s00163-020-00336-7.

Antonello, Federico, Buongiorno, Jacopo, Zio, Enrico, 2023a. Insights in the safety analysis of an early microreactor design. Nucl. Eng. Des. 404 (April). https://doi.org/10.1016/j.nucengdes.2023.112203.

Antonello, Federico, Buongiorno, Jacopo, Zio, Enrico, 2023b. Physics informed neural networks for surrogate modeling of accidental scenarios in nuclear power plants. Nucl. Eng. Technol. (September). https://doi.org/10.1016/j.net.2023.06.027.

Avramova, Maria N., Ivanov, Kostadin N., 2010. Verification, validation and uncertainty quantification in multi-physics modeling for nuclear reactor design and safety analysis. Prog. Nucl. Energy. https://doi.org/10.1016/j.pnucene.2010.03.009.

Arrieta, Barredo, Alejandro, Díaz-Rodríguez, Natalia, Del Ser, Javier, Bennetot, Adrien, Tabik, Siham, Barbado, Alberto, Garcia, Salvador, et al., 2020. Explainable artificial intelligence (XAI): concepts, taxonomies, opportunities and challenges toward responsible AI. Inf. Fusion 58 (June), 82–115. https://doi.org/10.1016/j.inffus.2019.12.012.

Benner, Peter, Gugercin, Serkan, Karen, Willcox, 2015. A survey of projection-based model reduction methods for parametric dynamical systems. SIAM Rev. 57 (4).

Betzler, Benjamin R., Chandler, David, Davidson, Eva E., Ilas, Germina, 2017. High-fidelity modeling and simulation for a high flux isotope reactor low-enriched uranium core design. Nucl. Sci. Eng. 187 (1), 81–99. https://doi.org/10.1080/00295639.2017.1292090.

Buongiorno, Jacopo, Carmichael, Ben, Dunkin, Bradley, Parsons, John, Smit, Dirk, 2021. Can nuclear Batteries Be economically competitive in large markets? Energies 14 (14).

Chaturantabut, Saifon, Sorensen, Danny C., 2010. Nonlinear model reduction via discrete empirical interpolation. SIAM J. Sci. Comput. 32 (5).

Conner, Landon, Worrell, Clarence L., Spring, James P., Liao, Jun, 2021. Machine learned metamodeling of a computationally intensive accident simulation code. In: Successes, and Lessons Learned; Nuclear Plant Engineering; Advanced Reactors and Fusion; Small Modular and Micro-reactors Technologies and Applications Proceedings of the 2021 28th International Conference on Nuclear Engineering, ume 1. Operating Plant Challenges.

Damianou, Andreas C., Neil, D. Lawrence, 2012. Deep Gaussian processes. November. http://arxiv.org/abs/1211.0358.

Dargan, Shaveta, Kumar, Munish, Ayyagari, Maruthi Rohit, Kumar, Gulshan, 2020. A survey of Deep learning and its applications: a new paradigm to machine learning. Arch. Comput. Methods Eng. 27 (4), 1071–1092. https://doi.org/10.1007/s11831-019-09344-w.

D'Auria, F., Camargo, C., Mazzantini, O., 2012. The best estimate plus uncertainty (BEPU) approach in licensing of current nuclear reactors. Nucl. Eng. Des. 248 (July), 317–328. https://doi.org/10.1016/j.nucengdes.2012.04.002.

D'Auria, Francesco Saverio, et al., 2009. Deterministic safety analysis for nuclear power plants. In: IAEA Specific Safety Guide, SSG-2. IAEA Safety Standards Series, Wien. Edited by IAEA.

Di Maio, F., Zio, E., Smith, C., Rychkov, V., 2015. Integrated deterministic and probabilistic safety analysis for safety assessment of nuclear power plants. Hindawi Publishing Corporation Science and Technology of Nuclear Installations 2.

Ebiwonjumi, Bamidele, Kong, Chidong, Zhang, Peng, Cherezov, Alexey, Lee, Deokjung, 2021. Uncertainty quantification of PWR spent fuel due to nuclear data and modeling parameters. Nucl. Eng. Technol. 53 (3), 715–731. https://doi.org/10.1016/j.net.2020.07.012.

Ebiwonjumi, Bamidele, Zhang, Peng, Lee, Deokjung, 2020. Sensitivity analysis of PWR spent fuel due to modelling parameter uncertainties using surrogate models. In: *International Conference on Physics of Reactors: Transition to a Scalable Nuclear Future, PHYSOR 2020*, 2020-March:2525–32. EDP Sciences - Web of Conferences. https://doi.org/10.1051/epjconf/202124715009.

El-Khatib, Hisham, El-Morshedy, Salah El Din, Higazy, Maher G., El-Shazly, Karam, 2013. Modeling and simulation of loss of the ultimate heat sink in a typical material testing reactor. Ann. Nucl. Energy 51 (January), 156–166. https://doi.org/10.1016/j.anucene.2012.07.031.

Feldman, E.E., Mohr, D., Chang, L.K., Planchon, H.P., Dean, E.M., Betten, P.R., 1987. EBR-II unprotected loss-of-heat-sink predictions and preliminary test results. Nucl. Eng. Des. 101.

Ghosh, Sandip, Saha, Samir Kumar, 2021. Modeling and simulation of subcooled coolant loss through circumferential pipe leakage. J. Nucl. Eng. Radiat. Sci. 7 (3). https://doi.org/10.1115/1.4048477.

Henry, A.F., 1958. The application of reactor kinetics to the analysis of experiments. Nucl. Sci. Eng. 3 (1), 52–70. https://doi.org/10.13182/nse58-1.

Herman, Elizabeth, Stewart, James A., Rémi, Dingreville, 2020. A data-driven surrogate model to rapidly predict microstructure morphology during physical vapor deposition. Appl. Math. Model. 88 (December), 589–603. https://doi.org/10.1016/j.apm.2020.06.046.

Hózer, Z., Adorni, M., Arkoma, A., Busser, V., Bürger, B., Dieschbourg, K., Farkas, R., et al., 2023. Review of experimental database to support nuclear power plant safety analyses in SGTR and LOCA domains. Annals of Nuclear Energy. Elsevier Ltd. https://doi.org/10.1016/j.anucene.2023.110001.

Hurtado, Jorge E., 2007. Filtered importance sampling with support vector margin: a powerful method for structural reliability analysis. Struct. Saf. 29 (1), 2–15. https://doi.org/10.1016/j.strusafe.2005.12.002.

Kang, Huilun, Tian, Zhaofei, Chen, Guangliang, Li, Lei, Wang, Tianyu, 2022. Application of POD reduced-order algorithm on data-driven modeling of rod bundle. Nucl. Eng. Technol. 54 (1), 36–48. https://doi.org/10.1016/j.net.2021.07.010.

Lek, S., Park, Y.S., 2008. Artificial neural networks. Encyclopedia of Ecology 237–245.

Liu, Shichang, Liang, Jingang, Yu, Jiankai, He, Qingming, Liu, Yang, 2023. Editorial: advanced modeling and simulation of nuclear reactors. Frontiers in Energy Research. Frontiers Media S.A. https://doi.org/10.3389/fenrg.2023.1189328.

Mathias, Marlon S., de Almeida, Wesley P., Coelho, Jefferson F., de Freitas, Lucas P., Moreno, Felipe M., Netto, Caio F.D., Cozman, Fabio G., et al., 2022. Augmenting a physics-informed neural network for the 2D burgers equation by addition of solution data points. In: Lecture Notes in Computer Science (Including Subseries Lecture Notes in Artificial Intelligence and Lecture Notes in Bioinformatics), 13654 LNAI. Springer Science and Business Media Deutschland GmbH, pp. 388–401. https://doi.org/10.1007/978-3-031-21689-3_28.

Maulik, Romit, Fukami, Kai, Ramachandra, Nesar, Fukagata, Koji, Taira, Kunihiko, 2020. Probabilistic neural networks for fluid flow surrogate modeling and data recovery. Physical Review Fluids 5 (10). https://doi.org/10.1103/PhysRevFluids.5.104401.

Mckay, M.D., Beckman, R.J., Conover, W.J., 1979. A Comparison of Three Methods for Selecting Values of Input Variables in the Analysis of Output from a Computer Code, vol. 21.

Memmott, Matthew, Buongiorno, Jacopo, Hejzlar, Pavel, 2010. On the use of RELAP5-3D as a subchannel analysis code. Nucl. Eng. Des. 240 (4), 807–815. https://doi.org/10.1016/j.nucengdes.2009.11.006.

Pedroni, Nicola, Zio, Enrico, 2017. An adaptive metamodel-based subset importance sampling approach for the assessment of the functional failure probability of a thermal-hydraulic passive system. Appl. Math. Model. 48 (August), 269–288. https://doi.org/10.1016/j.apm.2017.04.003.

Peterson, Janet S., 1989. The reduced basis method for incompressible viscous flow calculations. SIAM J. Sci. Stat. Comput. 10 (4).

Price, Dean, Radaideh, Majdi I., Kochunas, Brendan, 2022. Multiobjective optimization of nuclear microreactor reactivity control system operation with swarm and evolutionary algorithms. Nucl. Eng. Des. 393 (July). https://doi.org/10.1016/j.nucengdes.2022.111776.

Puppo, L., Pedroni, N., Di Maio, F., Bersano, A., Bertani, C., Zio, E., 2021. A framework based on finite mixture models and adaptive kriging for characterizing non-smooth and multimodal failure regions in a nuclear passive safety system. Reliab. Eng. Syst. Saf. 216 (December). https://doi.org/10.1016/j.ress.2021.107963.

Qian, Z., Seepersad, C.C., Joseph, V.R., Allen, J.K., Jeff Wu, C.F., 2005. Building surrogate models based on detailed and approximate simulations. J. Mech. Des. 128 (4), 668–677.

Radaideh, Majdi I., Tomasz, Kozlowski, 2020. Surrogate modeling of advanced computer simulations using Deep Gaussian processes. Reliab. Eng. Syst. Saf. 195 (March). https://doi.org/10.1016/j.ress.2019.106731.

Raissi, M., Perdikaris, P., Karniadakis, G.E., 2019. Physics-informed neural networks: a Deep learning framework for solving forward and inverse problems involving nonlinear partial differential equations. J. Comput. Phys. 378 (February), 686–707. https://doi.org/10.1016/j.jcp.2018.10.045.

Ryu, Seunghyoung, Kim, Hyeonmin, Kim, Seung Geun, Jin, Kyungho, Cho, Jaehyun, Park, Jinkyun, 2022. Probabilistic Deep learning model as a tool for supporting the fast simulation of a thermal–hydraulic code. Expert Syst. Appl. 200 (August). https://doi.org/10.1016/j.eswa.2022.116966.

Secchi, Piercesare, Zio, Enrico, Maio, Francesco Di, 2008. Quantifying uncertainties in the estimation of safety parameters by using bootstrapped artificial neural networks. Ann. Nucl. Energy 35 (12), 2338–2350. https://doi.org/10.1016/j.anucene.2008.07.010.

Stan, Marius, 2009. Discovery and design of nuclear fuels. Mater. Today. https://doi.org/10.1016/S1369-7021(09)70295-0.

Tripathy, Rohit K., Bilionis, Ilias, 2018. Deep UQ: learning Deep neural network surrogate models for high dimensional uncertainty quantification. J. Comput. Phys. 375 (December), 565–588. https://doi.org/10.1016/j.jcp.2018.08.036.

Unal, C., Williams, B., Hemez, F., Atamturktur, S.H., McClure, P., 2011. Improved best estimate plus uncertainty methodology, including advanced validation concepts, to license evolving nuclear reactors. Nucl. Eng. Des. 241, 1813–1833. https://doi.org/10.1016/j.nucengdes.2011.01.048.

Vedros, Kurt G., Christian, Robby, Otani, Courtney Mariko Yang Hui, 2022. Probabilistic Risk Assessment of a Light-Water Reactor Coupled with a High-Temperature Electrolysis Hydrogen Production Plant.

Worrell, Clarence, Luangkesorn, Louis, Haight, Joel, Congedo, Thomas, 2019. Machine learning of fire hazard model simulations for use in probabilistic safety assessments at nuclear power plants. Reliab. Eng. Syst. Saf. 183 (March), 128–142. https://doi.org/10.1016/j.ress.2018.11.014.

Wu, Xu, Kozlowski, Tomasz, 2017. Inverse uncertainty quantification of reactor simulations under the Bayesian framework using surrogate models constructed by

polynomial Chaos expansion. Nucl. Eng. Des. 313 (March), 29–52. https://doi.org/10.1016/j.nucengdes.2016.11.032.

Wuest, Thorsten, Weimer, Daniel, Irgens, Christopher, Thoben, Klaus Dieter, 2016. Machine learning in manufacturing: advantages, challenges, and applications. Production and Manufacturing Research 4 (1), 23–45. https://doi.org/10.1080/21693277.2016.1192517.

Yang, Chunlai, Xiaoguang, Hao, Zhang, Qijun, Chen, Heng, Yin, Zhe, Jin, Fei, 2023. Performance analysis of a 300 MW coal-fired power unit during the transient processes for peak shaving. Energies 16 (9). https://doi.org/10.3390/en16093727.

Yoon, Seok, Kim, Min Jun, Park, Seunghun, Kim, Geon Young, 2021. Thermal conductivity prediction model for compacted bentonites considering temperature variations. Nucl. Eng. Technol. 53 (10), 3359–3366. https://doi.org/10.1016/j.net.2021.05.001.

Zio, Enrico, Maio, Francesco Di, Tong, Jiejuan, 2010. Safety margins confidence estimation for a passive residual heat removal system. Reliab. Eng. Syst. Saf. 95 (8), 828–836. https://doi.org/10.1016/j.ress.2010.03.006.